Constrained spin-density functional theory for excited magnetic configurations in an adiabatic approximation

R. Singer and M. Fähnle
Max-Planck-Institut für Metallforschung, Heisenbergstr. 3, D-70569 Stuttgart, Germany

G. Bihlmayer
Institut für Festkörperforschung, Forschungszentrum Jülich, D-52425 Jülich, Germany
(Received 29 November 2004; revised manuscript received 15 April 2005; published 30 June 2005)

The magnetic energy and the magnitudes of the magnetic moments are calculated for excited magnetic configurations with strong moment cantings. The calculations are performed by use of an exact constraining scheme for the moments via constraining fields, and by use of an approximate constraining scheme via the prescription of the local spin quantization axes in the spin atomic sphere approximation. It is shown that the latter constraining scheme becomes totally inadequate for systems with strong moment cantings. When increasing the degree of moment canting, the magnitudes of the moments remain rather stable for Fe but become completely unstable for Ni while for Co the situation is in between the two cases.

DOI: 10.1103/PhysRevB.71.214435 PACS number(s): 75.10.−b, 71.15.Ap, 71.15.Mb

I. CONSTRAINING SCHEMES FOR EXCITED NONCOLLINEAR MAGNETIC CONFIGURATIONS

For the theory of magnetic excitations or of thermodynamic properties of magnetic materials often the adiabatic approximation is adopted. Thereby it is assumed that for the system under consideration the fast spin degrees of freedom from single-electron spin fluctuations on a time scale given by the inverse band width (typically 10^{-16} s) can be neglected and only the dynamics of the atomic moments $\mathbf{M}^\alpha$ on a time scale defined by the inverse frequencies of typical long-wavelength magnons (typically 10^{-14} s) are relevant.[1] We thereby define the atomic moment in the common way as an integral of the magnetic moment density $\mathbf{m}(\mathbf{r})$ over a suitably defined atomic volume Ω^α,

$$\mathbf{M}^\alpha = |\mathbf{M}^\alpha|\mathbf{e}^\alpha = \int_{\Omega^\alpha} \mathbf{m}(\mathbf{r}) d^3\mathbf{r}. \tag{1}$$

In the following we want to investigate the magnetic materials by the *ab initio* spin-polarized density functional theory[2] (DFT) where the energy of the system is represented as a functional of the charge density $n(\mathbf{r})$ and the magnetization density $\mathbf{m}(\mathbf{r}), E=E[n(\mathbf{r}),\mathbf{m}(\mathbf{r})]$, and where the ground state configuration is obtained by minimizing E with respect to $n(\mathbf{r})$ and $\mathbf{m}(\mathbf{r})$. Arbitrary excited magnetic states, however, in general do not correspond to stationary points of the energy hypersurface $E=E[n(\mathbf{r}),\mathbf{m}(\mathbf{r})]$. To calculate the energies at such nonstationary points in adiabatic approximation,[1] a static situation is generated by applying a constrained density functional theory where the directions e^α of the atomic moments are constrained to the nonequilibrium directions $\mathbf{e}_M^\alpha$. We denote the functional which has to be minimized subject to these constraints by $\tilde{E}[n(\mathbf{r}),\mathbf{m}(\mathbf{r})|\{\mathbf{e}_M^\alpha\}]$. In the literature there are two methods to construct this functional, a theoretically well founded constraining scheme (1) based on the use of Lagrangian parameters[3] and a simpler but only approximate[4] constraining scheme (2).

In this paper we will comment on the limitations of the calculational scheme (2): This scheme has been used quite often in the literature to describe systems with small cantings of the magnetic moments out of collinearity. One example is the calculation of the dispersion relations for spin waves in metallic systems via the energies of frozen-magnon configurations, i.e., of conical spin spirals with small cone-opening angles.[5,6] It has been shown[5] that in this situation the approximate scheme yields reliable results for systems with large exchange-correlation fields but it becomes inaccurate for systems with small exchange-correlation fields (see the discussion at the end of Sec. I). We now extend the discussion to situations with large spin cantings. Such situations are very important for the fast-growing field of nanomagnetism. Examples are domain walls in nanostripes[7] where the direction of the magnetization changes by 180° on an atomic scale. Other examples of probably even higher future technological relevance are the curl-like vortex magnetization configurations in nanoplatelets[8] where the system develops out-of-plane magnetization components to avoid a divergence of the magnetization gradient in the core of the vortex, or Bloch-point mediated processes for vortices.[9] Whereas continuum calculations based on the theory of micromagnetism[9] may be used to describe regions with small magnetization gradients, atomistic first-principles calculations are required[10] for regimes with large atomic-scale cantings. Because of the simplicity of the approximate calculational scheme and because of its success to describe the properties of spin waves in some materials it is thereby tempting to use it also for such systems with strong cantings. We will show, however, that it may become totally impractical in the latter systems. The approximate scheme is already quite often employed to the study of noncollinear magnetic systems in spite of the obvious superiority of the constraining field with Lagrangian parameters. The reason is that the constraining scheme (1) requires the implementation of

transverse magnetic fields in the code for noncollinear spin systems. (Having performed this implementation the additional computational cost required to determine the constraining field is very small.) We therefore think that our present paper represents an important guideline for the fast-growing community of people working on noncollinear spin systems.

In the following we consider calculations in which two approximations for the exchange-correlation energy E_{xc} of the DFT are used, namely the local-spin-density approximation[2] (LSDA), and in addition the atomic-sphere approximation for the spin direction[4] (spin ASA). In spin ASA, local spin quantization axes (SQAs) described by the unit vectors $\mathbf{e}_{\mathrm{SQA}}^{\alpha}$ are introduced, and for the calculation of E_{xc} only the projections $\mathbf{e}_{\mathrm{SQA}}^{\alpha}\cdot\mathbf{m}(\mathbf{r})$ of the magnetization density $\mathbf{m}(\mathbf{r})$ onto these axes are taken into account,

$$E_{\mathrm{xc}}^{\mathrm{ASA}}=\sum_{\alpha}\int_{\Omega^{\alpha}} n(\mathbf{r})\varepsilon_{\mathrm{xc}}[n(\mathbf{r}),\mathbf{e}_{\mathrm{SQA}}^{\alpha}\cdot\mathbf{m}(\mathbf{r})]d^{3}\mathbf{r}, \tag{2}$$

where $\varepsilon_{\mathrm{xc}}$ is the LSDA exchange-correlation energy per electron.[2]

In the constraining scheme (1) for the moment directions[3] local magnetic constraining fields $\mathbf{B}_{\mathrm{c}}^{\alpha}$ (which we take as constant in the respective volumes Ω^{α}, $\mathbf{r}$-dependent *Ansätze* are discussed in Refs. 11 and 12) are introduced which are perpendicular to the local magnetic moments $\mathbf{M}^{\alpha}=|\mathbf{M}^{\alpha}|\mathbf{e}^{\alpha}$ and which enforce that at the end of the self-consistent calculation of the DFT the quantities $\mathbf{M}^{\alpha}\times\mathbf{e}_{M}^{\alpha}$ vanish, i.e., that the moment directions $\mathbf{e}^{\alpha}$ are parallel to the desired directions $\mathbf{e}_{M}^{\alpha}$. The fields $\mathbf{B}_{\mathrm{c}}^{\alpha}$ play the roles of Lagrangian parameters in a generalized energy functional,

$$\begin{aligned}\tilde{E}[n(\mathbf{r}),\mathbf{m}(\mathbf{r})|\{\mathbf{e}_{M}^{\alpha}\},\{\mathbf{e}_{\mathrm{SQA}}^{\alpha}\}]&=E[n(\mathbf{r}),\mathbf{m}(\mathbf{r})|\{\mathbf{e}_{\mathrm{SQA}}^{\alpha}\}]\\&\quad+\sum_{\alpha}\mathbf{B}_{\mathrm{c}}^{\alpha}[\mathbf{e}_{M}^{\alpha}\times(\mathbf{M}^{\alpha}\times\mathbf{e}_{M}^{\alpha})],\end{aligned} \tag{3}$$

and thus have to be determined self-consistently. In Eq. (3) $E[n(\mathbf{r}),\mathbf{m}(\mathbf{r})|\{\mathbf{e}_{\mathrm{SQA}}^{\alpha}\}]$ is the usual LSDA energy functional in spin ASA for a given choice $\{\mathbf{e}_{\mathrm{SQA}}^{\alpha}\}$ of SQAs. In most calculations the SQAs for the next iteration step of the DFT calculation are chosen as being parallel to the moment directions from the preceding iteration step, so that at the end of the self-consistency cycle the local SQAs are parallel to the local magnetic moments (for another reasonable choice, see Ref. 5). It has been shown[11] that for this choice of the SQAs the quantities $-\mathbf{B}_{\mathrm{c}}^{\alpha}$ are identical to the transverse parts of the effective fields $\mathbf{B}_{\mathrm{eff}}^{\alpha}$ which would exert torques $\mathbf{B}_{\mathrm{eff}}^{\alpha}\times\mathbf{M}^{\alpha}$ on the magnetic moments in the configuration $\{\mathbf{e}_{M}^{\alpha}\}$ if the constraining fields were removed. These torques enter, e.g., the equation of motion[10,11] for the adiabatic variables $\mathbf{M}^{\alpha}$. In the following we denote the energy obtained by this procedure as $\tilde{E}[\{\mathbf{e}_{M}^{\alpha}\}]$.

The approximate constraining scheme (2) is based on the fact that in spin ASA the exchange-correlation fields $\mathbf{B}_{\mathrm{xc}}^{\alpha}$ are parallel to the directions $\mathbf{e}_{\mathrm{SQA}}^{\alpha}$ of the SQAs and favor an orientation $\mathbf{e}^{\alpha}$ of the magnetic moments close to the $\mathbf{e}_{\mathrm{SQA}}^{\alpha}$. On the other hand, the kinetic energy is minimum for a collinear magnetization density, and the competition between exchange-correlation energy and kinetic energy results in misalignment angles $\Delta\vartheta^{\alpha}$ between the $\mathbf{e}_{\mathrm{SQA}}^{\alpha}$ and the directions $\mathbf{e}^{\alpha}$ obtained by the spin ASA. Because the $\mathbf{B}_{\mathrm{xc}}^{\alpha}$ are often large, the hope is that the $\Delta\vartheta^{\alpha}$ are often small. The basic idea of the constraining scheme (2) therefore is to identify the $\mathbf{e}_{\mathrm{SQA}}^{\alpha}$ with the desired directions $\mathbf{e}_{M}^{\alpha}$ and to determine the directions $\mathbf{e}^{\alpha}$ from a minimization of $E[n(\mathbf{r}),\mathbf{m}(\mathbf{r})|\{\mathbf{e}_{\mathrm{SQA}}^{\alpha}=\mathbf{e}_{M}^{\alpha}\}]$, putting up with the hopefully small differences between $\mathbf{e}^{\alpha}$ and $\mathbf{e}_{M}^{\alpha}$. In the following we denote the energy obtained by this procedure as $E[\{\mathbf{e}^{\alpha}\}|\{\mathbf{e}_{\mathrm{SQA}}^{\alpha}=\mathbf{e}_{M}^{\alpha}\}]$. The effective fields $\mathbf{B}_{\mathrm{eff}}^{\alpha}$ acting on the magnetic moments in the configuration $\{\mathbf{e}^{\alpha}\}$ then are approximated by the quantities $\tilde{\mathbf{B}}_{\mathrm{eff}}^{\alpha}=1/|\mathbf{M}^{\alpha}|\,\partial E/\partial\mathbf{e}_{\mathrm{SQA}}^{\alpha}$.

It has been outlined in the literature (see, e.g., Ref. 11) that this approximate constraining scheme yields results for the densities $n(\mathbf{r})$ and $\mathbf{m}(\mathbf{r})$ which cannot be interpreted in a physically meaningful manner within the framework of the LSDA: A situtation where the $\mathbf{M}^{\alpha}$ are not parallel to the $\mathbf{e}_{\mathrm{SQA}}^{\alpha}$ and hence to the $\mathbf{B}_{\mathrm{xc}}^{\alpha}$ is—physically speaking—not stationary. The transverse components of $\mathbf{B}_{\mathrm{xc}}^{\alpha}$ exert a torque on $\mathbf{M}^{\alpha}$ and would lead[11,13] to a precission of the $\mathbf{M}^{\alpha}$ and hence to a dynamical situation which is not consistent with the static situation which we imply. In spite of this deficiency of the approximate constraining scheme it is often used in the literature (see above), hoping that the accuracy of the numerical data will be affected only slightly.

Numerical tests for the accuracy of the approximate constraining scheme are scarce. In Ref. 5 it has been shown for a frozen-magnon configuration with small cone-opening angle ϑ and wave vector $\mathbf{q}$ that the misalignment angles $\Delta\vartheta^{\alpha}$ scale like $\Delta\vartheta^{\alpha}/\vartheta\sim\omega(\mathbf{q})/|\langle\mathbf{B}_{\mathrm{xc}}\rangle|$ where $\langle\mathbf{B}_{\mathrm{xc}}\rangle$ is an appropriately averaged exchange-correlation field and $\omega(\mathbf{q})$ is the frequency of the magnon. For Fe with large $|\langle\mathbf{B}_{\mathrm{xc}}\rangle|$ this yields $\Delta\vartheta^{\alpha}/\vartheta<10\%$ whereas for Ni values up to 46% were found. In the present paper we extend the tests to the case of strong cantings of neighboring magnetic moments.

II. CALCULATIONAL PROCEDURE

Our calculations are based on the full-potential linearized augmented plane wave method[14] (FLAPW) as implemented in the FLEUR code,[12] and on the linear-muffin-tin-orbital method in atomic sphere approximation[15] which has been extended to the case of noncollinear spin systems.[16] In the latter code the system is subdivided into overlapping atomic spheres, and the ASA for the spin direction is performed everywhere. The FLEUR code is a "hybrid" code in the sense that the spin ASA is applied only in the muffin-tin spheres which are smaller than the overlapping atomic spheres (we use almost touching muffin-tin spheres) whereas it refrains from this approximation in the interstitial regimes between the muffin-tin spheres. Therefore the results from the FLAPW and the LMTO-ASA calculation will be different in general. We want to see whether the general statements obtained from a comparison of the calculations (1) and (2) are the same for FLAPW and LMTO-ASA.

To generate configurations with strong cantings of neighboring magnetic moments we consider supercells containing N atoms ($N=16$ for bcc Fe and hcp Co and $N=32$ for fcc Ni). We then calculate the energy E of the supercell and the magnitude $|\mathbf{M}^0|$ of the central atom ($\alpha=0$) by the following three procedures:

(A) We use the constraining scheme (1) and rotate the constraining field and hence the magnetic moment of the central atom by angles $\vartheta^0=\vartheta_M^0$ away from the z axis whereas all the other moments are enforced to be strictly parallel to the z axis. The curve interpolating between the discrete data points represents, the energy $\tilde{E}(\vartheta^0)$.

(B) We use the approximate constraining scheme (2) and rotate the SQA of the central atom by angles $\vartheta_{\mathrm{SQA}}^0=\vartheta^0$ away from the z axis while we fix the SQAs of all the other atoms in z direction ($\vartheta_{\mathrm{SQA}}^{\alpha\neq 0}=0$). As discussed above, the angles ϑ^α between the z axis and the final magnetic moments obtained by the LSDA calculation deviate from $\vartheta_{\mathrm{SQA}}^\alpha$ by $\Delta\vartheta^\alpha=\vartheta_{\mathrm{SQA}}^\alpha-\vartheta_M^\alpha$, the deviations possibly being strong for $\alpha=0$ and quite small for $\alpha\neq 0$. We then represent the data as a function of the final angle ϑ^0, and the curve interpolating between the discrete data points gives the energy $E(\vartheta^0)$.

(C) We use the constraining scheme (1) and enforce all moments into the directions of the final moments of calculation (B). Interpolating between the discrete data points yields the function $\tilde{E}'(\vartheta^0)$. Hence, the functions $\tilde{E}'(\vartheta^0)$ and $E(\vartheta^0)$ represent the energies for exactly the same respective spin configurations, once calculated by the exact constraining scheme and once by the approximate scheme (2). Because the noncentral moments deviate only very slightly from the z direction, the differences between $\tilde{E}'(\vartheta^0)$ and $\tilde{E}(\vartheta^0)$ are very small, and we therefore refrain from presenting the data from calculation (C) which are quite similar to the data from calculation (A).

We can compare the results of calculation (A) and (B) in two different ways. First, we can compare for the same input angles, i.e., $\vartheta_M^0=\vartheta_{\mathrm{SQA}}^0$, by comparing the respective nth data points of the two calculations. By this comparison we get an impression for the error which we make by approximating the true energy $\tilde{E}[\{\mathbf{e}_M^\alpha\}]$ by $E[\{\mathbf{e}^\alpha\}|\{\mathbf{e}_{\mathrm{SQA}}^\alpha=\mathbf{e}_M^\alpha\}]$. Second, we can compare for the same output angles $\tilde{E}[\{\mathbf{e}_M^\alpha\}]$ with $E[\{\mathbf{e}_M^\alpha\}|\{\mathbf{e}_{\mathrm{SQA}}^\alpha\neq\mathbf{e}_M^\alpha\}]$ considering the two latter quantities to be more similar than the two former quantities.

III. RESULTS

In the following we represent the results for the case of Fe, Co, and Ni. To facilitate the reading, we use throughout the whole Sec. III triangles or circles for the data from calculation (A) or (B), and full symbols or open symbols for the data from FLAPW and LMTO. Furthermore, we present the data first separately for Fe, Co and Ni in parts (a), (b) and (c) of the figures, respectively, and then we summarize the general results in the conclusions of Sec. IV.

The energy of the supercell (normalized to the energy for $\vartheta^0=0$), $\tilde{E}(\vartheta^0)$ and $E(\vartheta^0)$, is shown in Figs. 1(a)–1(c), and the magnitude of the central magnetic moment, $|\tilde{\mathbf{M}}^0(\vartheta^0)|$ and

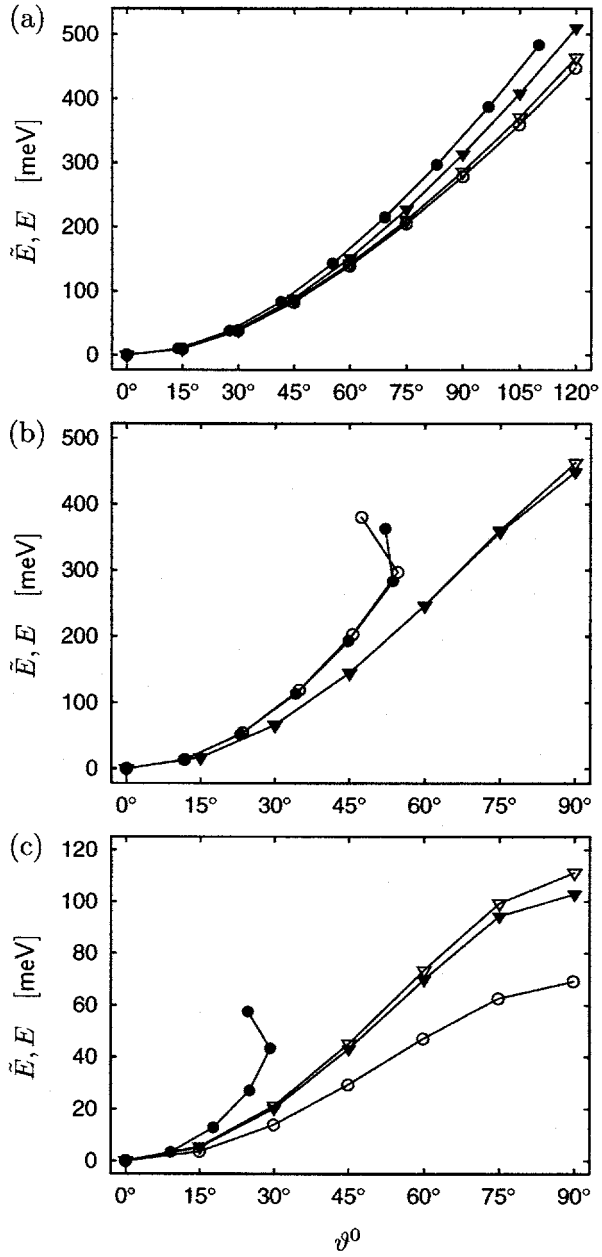

FIG. 1. The energy of the supercell, normalized to the energy for $\vartheta^0=0$, as function of the final angle ϑ^0 between the central moment and the z axis. Shown are the energies $\tilde{E}(\vartheta^0)$ (triangles) and $E(\vartheta^0)$ (circles) as obtained by the constraining scheme using constraining fields [calculational procedure (A), see Sec. II] and the approximate constraining scheme [calculational procedure (B)], respectively. Open symbols refer to LMTO, full symbols to FLAPW. (a) Fe; (b) Co; (c) Ni.

$|\mathbf{M}^0(\vartheta^0)|$, is shown in Figs. 2(a)–2(c). Note again that ϑ^0 refers to the output angle of the calculation, with $\vartheta^0=\vartheta_M^0$ for calculation (A) and $\vartheta^0\neq\vartheta_{\mathrm{SQA}}^0=\vartheta_M^0$ for calculation (B).

For the case of Fe the LMTO calculation (B) yields very small misalignment angles $\Delta\vartheta^0=\vartheta_{\mathrm{SQA}}^0-\vartheta^0$. This becomes obvious from the fact that the respective nth data points from calculation (A) and (B) appear almost at the same output angle ϑ^0. In contrast, the FLAPW calculation yields consid-

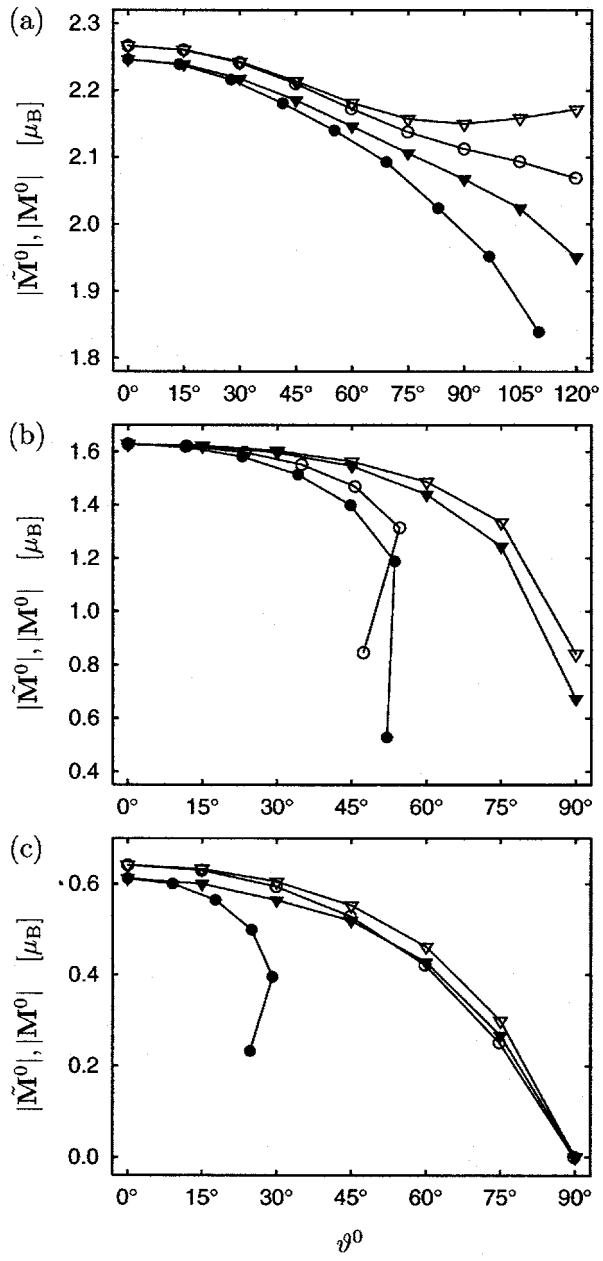

FIG. 2. The magnitude of the central magnetic moment as function of the final angle ϑ^0 between that moment and the z axis. Shown are the magnitudes $|\tilde{\mathbf{M}}^0(\vartheta^0)|$ (triangles) and $|\mathbf{M}^0(\vartheta^0)|$ (circles) as obtained by the constraining scheme using constraining fields [calculational procedure (A), see Sec. II] and the approximate constraining scheme [calculational procedure (B)], respectively. Open symbols refer to LMTO, full symbols to FLAPW. (a) Fe; (b) Co; (c) Ni. Note that the integration volumes for the moments $\mathbf{M}^\alpha$ are different for LMTO and FLAPW (see text).

erably larger misalignment angles. Our guess is that the difference arises because in the LMTO calculation the spin ASA is applied in the overlapping atomic spheres, whereas in FLAPW it is only applied in the smaller muffin-tin spheres, yielding a different competition between exchange energy and kinetic energy (see Sec. I). Whereas in LMTO the energies, Fig. 1(a), obtained from the two calculations are very similar there is a larger difference in FLAPW. Surprisingly, the agreement between the two energies is a bit better when we compare for the same input angle than when we compare for the same output angle. The magnitude of the central moment, Fig. 2(a), is reduced when increasing the output angle [apart from large output angles in the case of calculation (A), LMTO], the reduction being stronger in FLAPW than in LMTO [please note that the integration volume Ω^α in the definition of the magnetic moment via Eq. (1) is smaller for FLAPW (muffin-tin volume) than for LMTO (atomic-sphere volume)].

For the case of Co the misalignment angles are much larger than for Fe, both in LMTO and in FLAPW. Obviously in Co the influence of the kinetic energy which favors a parallel alignment of the various magnetic moments is stronger than in Fe. For large ϑ^0 the functions $E(\vartheta^0)$, Fig. 1(b), and $|\mathbf{M}^0(\vartheta^0)|$, Fig. 2(b), are not even unique. The reason is that the exchange-correlation field [for which only the projection of the magnetization on the SQA is relevant in spin ASA, see Eq. (2)], which tries to rotate the magnetic moment in the direction of the SQA gets smaller and smaller when the moment lags more and more behind the SQA. Finally, with further increase of ϑ^0 a backward rotation of the moments becomes energetically more favorable. As a result, two different values $\vartheta^0_{\mathrm{SQA}}$ generate the same output angle ϑ^0. The energies for the two situations are of course different because the respective exchange-correlation energies according to Eq. (2) are calculated from the projections of the magnetization density on two different SQAs. The magnitude of the central moment is more reduced than in Fe when increasing ϑ^0. The FLAPW calculation yields a reduction from about 1.8 μ_B for the ferromagnetic alignment to about 0.65 μ_B for a 90° orientation. The results from LMTO and FLAPW agree very well for the energies and a little bit less well for the magnitudes of the central moment.

For the case of Ni we get very different results from LMTO and FLAPW. For LMTO the misalignment angles are very small and comparable to those which we found for Fe. This is surprising because for the frozen-magnon configurations with small cone-opening angle (i.e., small canting of the magnetic moments) the misalignment angles are considerably larger[5] than for Fe (see Sec. I). However, one must take into account that a frozen-magnon configuration represents a continuous rotation of the moment direction from atom to atom whereas in the present calculation only the central moment is rotated while all the other 31 moments in the supercell are fixed in z direction. For FLAPW, however, the misalignment angles become very large and the functions $E(\vartheta^0)$, Fig. 1(c), and $|\mathbf{M}^0(\vartheta^0)|$, Fig. 2(c), are no longer unique even at rather small values of ϑ^0. The reason for this discrepancy between LMTO and FLAPW is probably related to the fact that for Ni the magnetization density is less localized than for Fe so that it leaks into the interstitial regimes of the FLAPW method where the spin ASA is not applied. The magnitude of the central moment as obtained in calculation (A) totally vanishes for a 90° orientation, both in LMTO and in FLAPW (see also Refs. 17 and 18).

Altogether, we can conclude that when increasing the degree of spin canting the magnitudes of the magnetic moments remain rather stable in Fe whereas they become very

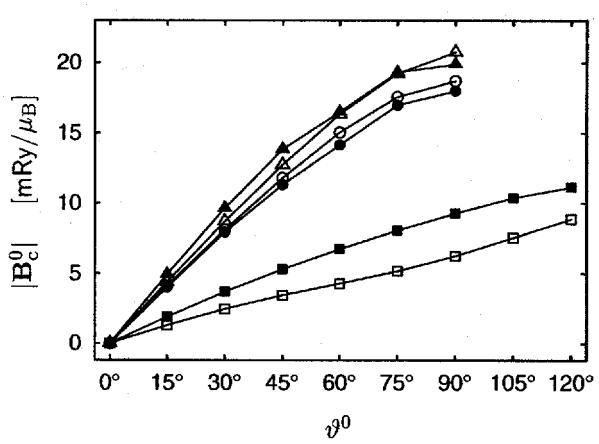

FIG. 3. The magnitude $|\mathbf{B}_c^0|$ of the constraining fields at the central magnetic moment for Fe (squares), Co (triangles), and Ni (circles) as obtained by FLAPW (full symbols) and LMTO (open symbols).

unstable for Ni. This reveals a totally different physical behavior of Fe and Ni which has to be taken into account when interpreting experimental data for noncollinear spin configurations in these systems. The results also clearly demonstrate that magnetism in Ni can by no means be described by the Heisenberg model which assumes constant magnitudes of the moments. This deficiency of the Heisenberg model has been discussed for Fe and Ni already in the paper of Turzhevskii *et al.*[18] who found a dependence of the magnitude of the magnetic moment on the degree of spin canting similar to the one which we obtained. According to our results the behavior of Co is in between the situations for Fe and Ni. Although its deficiency is known, the Heisenberg model is still used frequently to model the spin dynamics in empirical simulations. A more appropriate representation of the adiabatic magnetic energy hypersurface for systems with arbitrary spin cantings and stable or unstable magnetic moments is provided by the recently developed spin cluster expansion.[10,19] Naturally, when encountering nonadiabatic situations as, e.g., finite-temperature itinerant magnetism, more advanced methods have to be applied (see, e.g., Ref. 20).

Finally, in Fig. 3 we compare the magnitudes $|\mathbf{B}_c^0|$ of the constraining fields as obtained by FLAPW and by LMTO. For Co and Ni the two calculations yield very similar constraining fields whereas for Fe the differences are a bit larger.

IV. SUMMARY AND CONCLUSIONS

In the present paper we compared the results for excited noncollinear magnetic configurations which were generated by a constraining scheme based on constraining fields and by an approximate scheme which tries to prescribe the moment directions by fixing the directions of the local spin quantization axes (SQAs) accordingly. In the latter method there are misalignments between the final moment directions and the directions of the SQAs which define the directions of the exchange-correlation field. The problems arising from these misalignments have been discussed in the literature by general theoretical arguments. In spite of these problems, the approximate constraining scheme is still used in the literature (probably because it does not require the implementation of transverse fields in the band-structure codes) hoping that the numerical errors are small. So far these numerical errors have been investigated[5] only for frozen-magnon configurations with small cantings of the magnetic moments. In the present paper we have extended the numerical investigations to strong spin cantings. It has been shown that—depending on the electronic structure of the material—the use of the approximate constraining scheme becomes totally impractical, mainly because of the following three reasons.

(1) The misalignment angles may become very large so that the SQAs no longer characterize the configurations of the moments appropriately.

(2) For large cantings the magnetic energy is no longer necessarily a unique function of the orientations of the SQAs or a unique function of the final moment configuration.

(3) Band-structure calculations employing different approximations to the representation of the vector magnetization density may yield drastically different results. In constrast, when constraining the moment directions via constraining fields the results from different band-structure calculations in general agree rather well.

To conclude, we have shown that for an investigation of systems with strong atom scale cantings of the magnetic moments, the use of the exact constraining scheme via constraining fields is absolutely essential.

[1] B. L. Gyorffy, A. J. Pindor, J. Staunton, G. M. Stocks, and H. Winter, J. Phys. F: Met. Phys. **15**, 1337 (1985).
[2] U. von Barth and L. Hedin, J. Phys. C **5**, 1629 (1972).
[3] P. H. Dederichs, S. Blügel, R. Zeller, and H. Akai, Phys. Rev. Lett. **53**, 2512 (1984).
[4] H. Köhler, J. Sticht, and J. Kübler, Physica B **172**, 79 (1991).
[5] O. Grotheer, C. Ederer, and M. Fähnle, Phys. Rev. B **63**, 100401(R) (2001).
[6] S. V. Halilov, H. Eschrig, A. Y. Perlov, and P. M. Oppeneer, Phys. Rev. B **58**, 293 (1998).
[7] M. Pratzer, H. J. Elmers, M. Bode, O. Pietzsch, A. Kubetzka, and R. Wiesendanger, Phys. Rev. Lett. **87**, 127201 (2001).
[8] J. Miltat and A. Thiaville, Science **298**, 555 (2002).
[9] A. Thiaville, J. M. Garcia, R. Dittrich, J. Miltat, and T. Schrefl, Phys. Rev. B **67**, 094410 (2003).
[10] M. Fähnle, R. Drautz, R. Singer, D. Steiauf, and D. V. Berkov, Comput. Mater. Sci. **32**, 118 (2005).
[11] G. M. Stocks, B. Ujfalussy, X. D. Wang, D. M. C. Nicholson, W. A. Shelton, Y. Wang, A. Canning, and B. L. Gyorffy, Philos. Mag. B **78**, 665 (1998).
[12] Ph. Kurz, F. Förster, L. Nordström, G. Bihlmayer, and S. Blügel, Phys. Rev. B **69**, 024415 (2004).

[13] L. M. Small and V. Heine, J. Phys. F: Met. Phys. **14**, 3041 (1984).
[14] E. Wimmer, H. Krakauer, M. Weinert, and A. J. Freeman, Phys. Rev. B **24**, 864 (1981).
[15] O. K. Andersen and O. Jepsen, Phys. Rev. Lett. **53**, 2571 (1984).
[16] M. Liebs, K. Hummler, and M. Fähnle, Phys. Rev. B **51**, 8664 (1995); O. Grotheer and M. Fähnle, Phys. Rev. B **59**, 13965 (1999).
[17] V. Heine, A. I. Lichtenstein, and O. N. Mryasov, Europhys. Lett. **12**, 545 (1990).
[18] S. A. Turzhevskii, A. I. Lichtenstein, and M. I. Katsnelson, Sov. Phys. Solid State **32**, 1138 (1990).
[19] R. Drautz and M. Fähnle, Phys. Rev. B **69**, 104404 (2004).
[20] A. I. Lichtenstein, M. I. Katsnelson, and G. Kotliar, Phys. Rev. Lett. **87**, 067205 (2001).